

Analysis of Combustibility Limits for Lean Methane/Air Mixtures in Cylindrical Annular Packed Bed

VALERI BUBNOVICH, LUIS HENRÍQUEZ-VARGAS

Department of Chemical Engineering,
Universidad de Santiago de Chile,
B. O'Higgins 3363, Santiago,
CHILE.

valeri.bubnovich@usach.cl; www.usach.cl

Abstract:- A numerical study by means of computational simulations in COMSOL Multiphysics of a lean methane/air mixture in a porous media burner is performed using a novel geometry of a cylindrical annular space for combustion to be developed in. A two-dimensional mathematical model for filtration combustion is used to estimate the lean combustibility limits (*LCL*), as function of gas inlet velocity and composition and different dimensions of the inner cylinder radius. The porous media used is made up of 5.6 mm diameter alumina balls forming a porosity whose value is about 0.4. The burner outer cylinder is insulated and the inner cylinder considers convective heat losses with heat transfer coefficient values in the range $800 < h < 1500$, W/m^2 . The simulation focuses on the two-dimensional temperature analysis and displacement dynamics of the combustion front inside the reactor, depending on the values of the filtration velocity ($0.1 < u_{g0} < 1.0$, m/s) and the fuel equivalence ratio ($\Phi < 0.5$) for two values of the internal cylinder radius, 0.01 and 0.02 m.

Key Words: Porous media, gas combustion, combustibility limits

1. Introduction

The need to lower emissions and increase efficiency in fossil fuel combustion has driven the search of new combustion methods and advanced burner designs. A porous media burner can provide a good solution due to a number of advantages compared to conventional free-flame combustion, such as large power variation range, high efficiency, compact structure with very high energy concentration per unit volume, extremely low *CO* and *NO_x* emissions over a wide range of thermal loads, stable combustion over a wide range of equivalence ratios, $0.4 < \Phi < 0.9$ [1–3]. All the arguments mentioned above have driven the current development of these kinds of burners which have already found several important industrial applications [4–7]. The problem of gas combustion in inert porous media has been studied intensively both theoretically and experimentally. The most important results of both research methodologies have been summarized in [8, 9]. One of the most important problems of porous media burners is stabilizing the flame in a specific zone of the inert porous media. It is also important for the static combustion front to have some predefined characteristics to be able to

maximize the efficiency of the burner and minimize *CO* and *NO_x* emissions [2, 3, and 5]. For this purpose, four different flame control methods have been developed. The first method considers forming two layers of the porous media in which the modified Peclet number is less than (first layer) or greater than (second layer) 65 [1–3, 8, 10–12]. The second method considers cooling the post-combustion zone [13, 14]. The third method enables retaining the flame in a specific zone of the porous media by periodically exchanging the mixture inlet and exhausting the combustion gases [15–19]. Finally, the fourth method of flame stabilization employs a porous body with non-constant cross sectional area [20]. The motion of the combustion zone results in positive or negative enthalpy fluxes between the reacting gas and solid porous media. As a result, observed combustion temperatures can significantly differ from adiabatic predictions based on the enthalpy of the initial reactants and is controlled mainly by reaction chemistry and heat transfer mechanism. Upstream wave propagation against the gas flow results in subadiabatic combustion temperature, while downstream propagation of the wave leads to combustion in the superadiabatic regime, with much higher

temperatures than the adiabatic temperature [21-23]. Superadiabatic combustion significantly extends conventional flammability limits to the region of ultralow heat content mixtures.

For an adequate burner design with a specific porous media, it is imperative to know the temperature levels reached and the travel speed of the combustion front inside the porous media according to several parameters. These parameters include the physical properties of the porous media, gas filtration speed and fuel equivalence ratio, amongst others. The main results published on this subject may be found in [8, 10, 12, 21, 23 and 24]. According to investigations, the combustion front velocity is positive (front moves downstream) in the ultra-poor ($\Phi \rightarrow 0$) mixtures and is negative in mixtures close to stoichiometric ($\Phi \rightarrow 1$) throughout the range of variation of the speed gas filtration. However, for lean mixtures, i.e., those with Φ values that lie between the two extremes mentioned above, there is normally a theoretical value of the filtration gas velocity u_g^* for which $u_{FC} = 0$. As a result, for $u_g > u_g^*$, $u_{FC} > 0$ and for $u_g < u_g^*$, $u_{FC} < 0$. Moreover, the value of u_g^* increases for higher values of Φ . However, with the increased value of Φ , the positive values of u_{FC} decrease their size and the negative values of u_{FC} grow. Exactly the same is observed with increasing pore diameter of the porous medium.

The literature review shows that the combustion in inert porous media with cylindrical annular geometry was not investigated practically. For this reason, it is interesting to ask: What properties will the combustion of methane/air lean mixtures in burners with this type of geometry have? Will these properties be different from those of combustion in the cylindrical geometry? Answers to these questions what are sought in this paper.

2. Physical Situation

The burner analyzed in this work is made of two stainless steel tubes of different diameters, one placed inside the other, with its annular space filled with alumina balls, as shown in Figure 1. The external cylinder of the burner is insulated, while the interior cylinder has interfacial energy losses from the reactor to the cylindrical space in the middle of the burner where a coolant fluid circulates. The combustion of the lean fuel gaseous mixture takes place in the annular space filled by the porous media. The mixture is ignited in the region located at half the height of the reactor, imposing the initial ignition temperature there. As a result,

combustion front moves along the reactor upstream or downstream, depending on the physical conditions assigned to four different variables: gas filtration rate, fuel equivalence ratio, heat loss from the internal cylinder of the burner and the radius of the cylinder itself. Combustion development is analyzed for each combination of these four parameters, including the combustion front velocity and the two-dimensional transient temperature profiles that are generated.

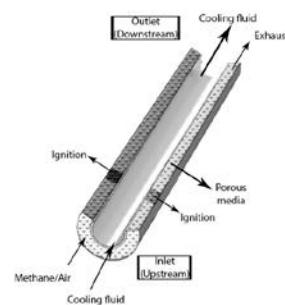


Fig. 1: Burner diagram

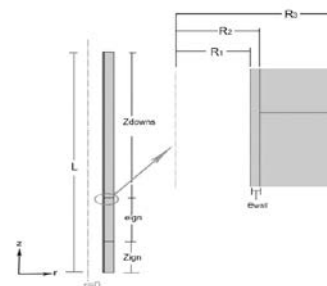
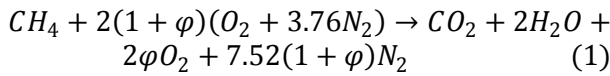


Fig. 2: Burner diagram used in computer simulations

The porous media annular burner schematic is shown in Figure 1, along with its geometry in Figure 2, for its application in computer simulations. As seen here, the system is made up of two cylinders of length L . Since the external cylinder of radius R_3 is insulated, its wall thickness is not considered here. The internal cylinder of the burner, with wall thickness given by $R_2 - R_1 = e_{wall}$, exchanges heat both with the annular porous media and the coolant fluid circulating in the middle cylindrical space. The whole volume of the burner is made up of three regions. The first one, called “Upstream” is of Z_{ign} length and belongs to the entrance area of the methane/air mixture. A second region, of length e_{ign} , called the ignition region, is where the chemical reaction begins and develops. The third region, of length Z_{downs} , called “Downstream,” is that where the combustion products are released. The whole region of height L and width $R_3 - R_2$ will be filled with 5.6 mm diameter alumina balls.

3. Mathematical Model

The mathematical model presented below, which is made up of equations governing the combustion process of lean methane/air mixtures in porous media according to the global reaction:



Where φ is the excess air coefficient of the mixture that has the following relation with the fuel equivalence ratio Φ :

$$\Phi = 1/(1 + \varphi) \quad (2)$$

When using a compressible fluid, the conservation of mass is given by:

$$\frac{\partial \rho_g}{\partial t} + \nabla \cdot (\rho_g \mathbf{u}_g) = 0 \quad (3)$$

Where \mathbf{u}_g represents the gas filtration velocity and gas density ρ_g is governed by the law of ideal gas:

$$\rho_g = \frac{pM_g}{RT_g} \quad (4)$$

Where p represents gas pressure, $R = 8.314 \text{ J/(mol K)}$ is the universal constant of gases, T_g is the temperature of the gas phase and M_g is the molar mass of the mixture that is a function of Φ . The equation of fuel mass conservation, considering single step kinetics is given by:

$$\frac{\partial c}{\partial t} + \mathbf{u}_g \cdot \nabla c = \nabla \cdot (D \nabla c) - Ace^{\frac{-E_a}{RT_g}} \quad (5)$$

Where c is the methane concentration in mol/m^3 , $A = 2.6 \cdot 10^8 \text{ [1/s]}$ is the frequency factor, $E_a = 1.3 \cdot 10^5 \text{ [J/mol]}$ is the activation energy and D is the effective diffusion tensor of the mixture in m^2/s , which considers both, the contribution by molecular diffusion (D_g) and dispersion (D_d) [23]:

$$D = D_g \mathbf{I} + D_d \quad (6)$$

The dispersion tensor coefficient is given by:

$$D_d = \begin{bmatrix} D_p \tau_z^2 + D_t \tau_z^2 & (D_p - D_t) \tau_z \tau_r \\ (D_p - D_t) \tau_z \tau_r & D_p \tau_z^2 + D_t \tau_z^2 \end{bmatrix} \quad (7)$$

Where τ_z and τ_r represent the normalized axial and radial components of the velocity vector:

$$\tau = \frac{\mathbf{u}_g}{|\mathbf{u}_g|} \quad (8)$$

The parallel D_p and transversal D_t components of the dispersion tensor D_d are defined [1] as:

$$D_p = 0.5d_p |\mathbf{u}_g| \quad (9)$$

$$D_t = 0.1d_p |\mathbf{u}_g| \quad (10)$$

Where d_p is the pore diameter. The energy conservation equation for the fluid phase is expressed as:

$$\rho_g C p_g \frac{\partial T_g}{\partial t} + \rho C p_g \mathbf{u}_g \nabla T_g = \nabla \cdot (\mathbf{k} \cdot \nabla T_g) + Ace^{\frac{-E_a}{RT_g}} \cdot \Delta h_m - \frac{\alpha_{vol}}{\varepsilon} \cdot (T_g - T_s) \quad (11)$$

Where $\Delta h_m = 847000 \text{ J/mol}$ is the molar heat of the chemical reaction and ε represents the porosity of the porous matrix. The physical properties of the fluid are approximated to air [4]:

$$\mathbf{k} = k_g + 0.5\rho_g C_p d_p \mathbf{u}_g \quad (12)$$

$$C p_g = 947e^{1.83 \cdot 10^{-4} T_g} \quad (13)$$

$$k_g = 4.82 \cdot 10^{-7} C p_g T_g^{0.7} \quad (14)$$

$$\mu_g = 3.37 \cdot 10^{-7} T_g^{0.7} \quad (15)$$

Where k_g is the thermal conductivity, μ_g is the dynamic viscosity and $C p_g$ is the specific heat capacity of the gas phase, respectively. As noted, effective gas conductivity includes both thermal conductivity and its dispersion component. In the same equation (11) α_{vol} is the volumetric heat transfer coefficient between the solid and liquid phases [2, 3]:

$$\alpha_{vol} = \frac{6k_g(1-\varepsilon)}{d_p^2} (2 + 1.1Pr^{1/3} Re^{0.6}) \quad (16)$$

Where Pr and Re are the dimensionless numbers of Prandtl and Reynolds:

$$Pr = \frac{\mu_g C p_g}{k_g} \quad (17)$$

$$Re = \frac{\rho_g \varepsilon |\mathbf{u}_g| d_p}{\mu_g} \quad (18)$$

The energy conservation equation for the porous media:

$$(1 - \varepsilon) \rho_s C p_s \frac{\partial T_s}{\partial t} = \nabla \cdot (k_{s\text{eff}} \nabla T_s) + \frac{\alpha_{vol}}{\varepsilon} (T_g - T_s) \quad (19)$$

Where $\rho_s = 3987 \text{ kg/m}^3$ is the alumina density and $k_{s\text{eff}}$ is the effective thermal conductivity of the porous media considering the conductive and radiative transport mechanisms, respectively, according to the Rosseland approximation [5]:

$$k_{s\text{eff}} = F_C (1 - \varepsilon) k_s + \frac{32 \sigma d_p \varepsilon \varepsilon_m}{9(1-\varepsilon)} T_s^3 \quad (20)$$

Where $F_C = 0.01$ is the contact factor between the alumina balls, ε_m is the emissivity of the porous

Table 1: Values of the four variables

	Values	Units
u_{g0}	0.1, 0.3, 0.5, 0.7, 1.0	[m/s]
Φ	0.1, 0.2, 0.3, 0.4, 0.5	
h_{cool}	400, 800, 1500	[W/m ² ·K]
R_1	0.01, 0.02	[m]

For each of the four variables analyzed, we have created four different graphics representing the values of the combustion front velocity in the porous media, the temperatures along the external cylinder ($r = R_3$) and the internal cylinder ($r = R_1$ and $r = R_2$), and the minimum values of the fuel equivalence ratio (Φ_{min}) at which the combustion in the annular space does not extinguish (combustibility limits), depending on the gas filtrating speed. The analysis of these cases is done in the following order. First, $R_1 = 0.01\text{ m}$ is chosen for three different values of h_{cool} presented in Table 1 and the wave properties of combustion determined by u_{g0} and Φ are analyzed. Then, the same analysis is applied to the case with $R_1 = 0.02\text{ m}$.

Figures 3 – 6 show the case of $R_1 = 0.01\text{ m}$ and $h_{cool} = 400\text{ W/m}^2/\text{K}$. Figure 3 shows that in the five cases analyzed by Φ , for $\Phi = 0.1, 0.2$ and 0.3 , the combustion wave moves downstream at a velocity whose order of magnitude is 10^{-4} m/s , reaching a superadiabatic regime. In cases of $\Phi = 0.4$ and 0.5 , the wave moves upstream in a subadiabatic regime. Something similar occurs with combustion wave movements in porous cylindrical media: increasing the value of Φ changes the superadiabatic regime to subadiabatic. However, a notorious change is also observed in the $u_{FC} = f(u_{g0})$ functionality for any value of Φ : the almost straight lines located absolutely above or below the horizontal axis of u_{g0} in the case of annular geometry (see figures 3, 8, 10 and 12) are changed for downward concave curves that cross axis u_{g0} at some point in circular geometry [10]. In short, for a fixed Φ , the u_{FC} combustion front velocity keeps the same sign (travel direction) regardless of the value of u_{g0} . Also, in all the cases, the combustion front velocity increases as the gas filtration velocity increases, for the same values of Φ .

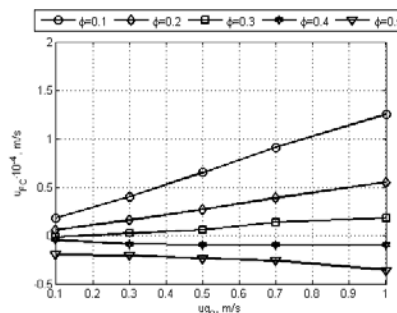


Fig. 3: Combustion front velocity as function of gas entry velocity and equivalence ratio, $R_1 = 0.01\text{ m}$ and $h_{cool} = 400\text{ W/m}^2/\text{K}$.

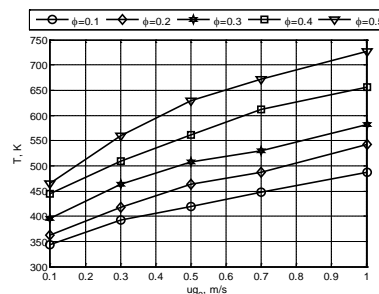


Figure 4: Solid maximum temperatures as function of gas entry velocity and equivalence ratio, $R_1 = 0.01\text{ m}$ and $h_{cool} = 400\text{ W/m}^2/\text{K}$.

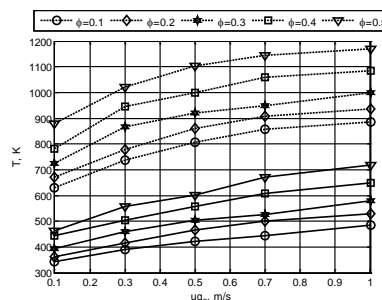


Figure 5: Maximum temperatures of gas (dotted line) and solid (solid line) in $R_2 = 0.012\text{ m}$ as function of gas entry velocity and equivalence ratio, $R_1 = 0.01\text{ m}$ and $h_{cool} = 400\text{ W/m}^2/\text{K}$.

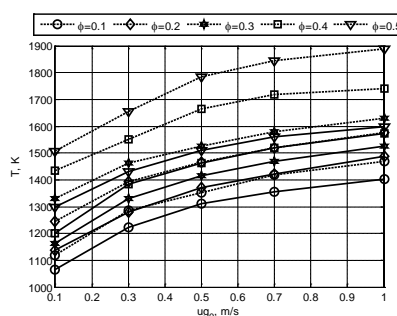


Figure 6: Maximum temperatures of gas (dotted line) and solid (solid line) in $R_3 = 0.038\text{ m}$ as function of gas entry velocity and equivalence ratio, $R_1 = 0.01\text{ m}$ and $h_{cool} = 400\text{ W/m}^2/\text{K}$.

Figures 4 – 6 show the maximum temperatures reached on different solid surfaces of the annular cylindrical burner: on external ($R_1 = 0.01\text{ m}$) and internal ($R_2 = 0.012\text{ m}$) surfaces of the internal cylinder and on the internal surface of the external cylinder ($R_3 = 0.038\text{ m}$), respectively. Figure 4 shows that the highest temperatures reached on the cooled

surface of the internal cylinder ($r = R_1$) is within the range of $350 < T_s < 750K$, for the analyzed values of Φ and $u_{g,0}$. On the other hand, according to figure 5, the temperatures of the solid and the gas in $R_2 = 0.012m$ (porous media in contact with the internal surface of the same cylinder) remains within the ranges of $350 < T_s < 700K$ and $600 < T_g < 1200K$, respectively, indicating that this location does not have local thermal equilibrium: on average, $T_g - T_s \sim 400K$. For higher values of gas filtration velocity and equivalence ratio, the maximum temperatures for both gas and solid increased. Figure 6 shows that the highest temperatures of gas and solid reached in the porous media that is in contact with the insulated surface of the external cylinder of the burner is located at intervals $1100 < T_g < 1900K$ and $1050 < T_s < 1600K$, respectively. A local thermal non equilibrium in this area is also observed, where the local differences $T_g - T_s$ are in the range between 100 and 200 K, with greater differences for higher values of Φ .

Finally, figure 7 shows the combustibility limits according Φ_{min} values, depending on the input gas velocity $u_{g,0}$. The figure shows that these limits decrease from 0.1 up to 0.06 when the gas velocity $u_{g,0}$ increases its value from 0.1 to 1.0 m/s. Also, the same figure shows the highest temperatures reached by the porous media (three marked lines) and the gas (two unmarked lines) located in contact with the cooled surface of the internal cylinder (one dotted line, $r = R_1$), also on the internal surface of the same cylinder (two broken lines, $r = R_2$) and on the surface of the external cylinder (two solid lines, $r = R_3$). As seen in the figure, the temperatures of all the surfaces gradually increase with the increase of Φ . Gas temperatures of the insulated cylinder surface come near to 1500K, while solid temperature, on average, border 1250K. On the other hand, on the surface $r = R_2$, gas temperature is in the range 600 to 775K, showing higher values for higher Φ , while temperatures of the solid phase in the same location are around 500K, practically matching the temperatures of the cylinder itself, but on the cooled side, $r = R_1$ (in the figure these two lines concur).

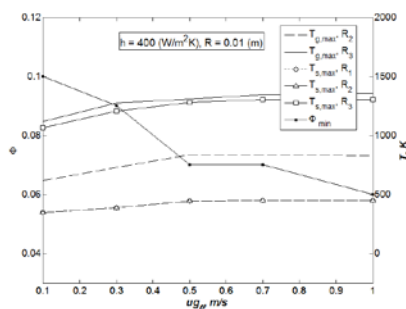


Figure 7: Combustibility limits (values of Φ_{min}) and maximum gas (dotted lines) and solid (solid lines) temperatures within the reactor in R_1, R_2 y R_3 : $R_1 = 0.01m$ and $h_{cool} = 400 W/m^2/K$.

After analyzing the case with $R_1 = 0.01m$ and $h_{cool} = 400 W/m^2/K$, the value of h_{cool} was varied, first to $h_{cool} = 800 W/m^2/K$ and later to $h_{cool} = 1500 W/m^2/K$, for the same value of R_1 . Results showed that both the combustion front velocity and the combustibility limits of the mixture remained practically invariable, therefore the intermediate case $h_{cool} = 800 W/m^2/K$ was omitted in the illustration, showing only the case with $h_{cool} = 1500 W/m^2/K$ in figures 8 and 9. These figures show that the combustion front velocity, combustibility limits and temperatures of the insulated cylinder surface ($r = R_3$) did not actually suffer a noticeable change in their values. However, some changes in values of temperature are seen near the interior cylinder: both the temperatures of the gas and the solid have decreased by an average of $75^\circ C$ on the surface $r = R_2$, just like the temperatures on the cooled surface in $r = R_1$.

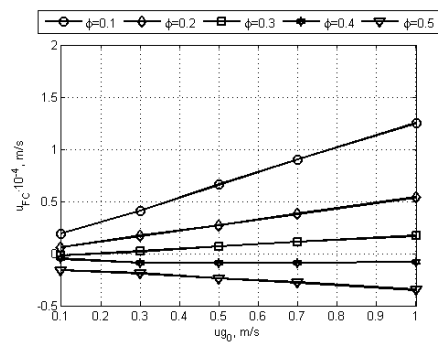


Figure 8: Combustion front velocity as function of gas entry velocity and equivalence ratio, $R_1 = 0.01m$ and $h_{cool} = 1500 W/m^2/K$.

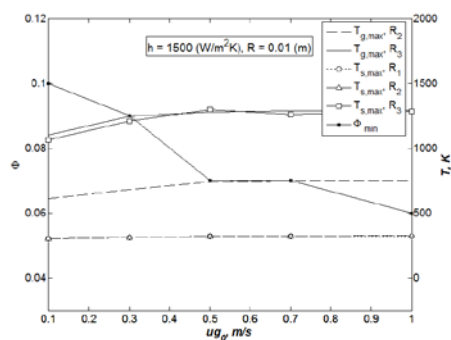


Figure 9: Combustibility limits (values of Φ_{min}) and maximum temperatures of gas (dotted lines) and solid (solid lines) within the reactor in R_1, R_2 y R_3 : $R_1 = 0.01m$ and $h_{cool} = 1500 W/m^2/K$.

Finally, the same analysis as above was repeated for the variation of $u_{g,0}$, h_{cool} and Φ , according to Table 1, but now with $R_1 = 0.02 m$. For example, comparing figure 3 with 10 and 8 with 11, respectively, the influence of the change of the inner cylinder radius R_1 can be analyzed for the same

value of $h_{cool} = 400 \text{ W/m}^2/\text{K}$. Figures 3 and 10 show that with the increase in the value of R_I from 0.01 to 0.02m, the combustion front velocity for the cases of $\Phi = 0.1, 0.2$ and 0.3, noticeably increased their values, by up to 40% for $\Phi = 0.1$, keeping the superadiabatic regime seen in figure 3. The same figure also shows that in the case $\Phi = 0.1$, the stable combustion waves of the system only exist in the interval of gas entry velocity between 0.5 and 1.0 m/s. For lower values of u_{g0} , combustion does not occur and it is extinguished. On the other hand, in the subadiabatic regime with $\Phi = 0.4$ and 0.5, the changes in the values of the combustion front velocity are much smaller, up to 10% and no qualitative changes are observed in figures 3 and 10.

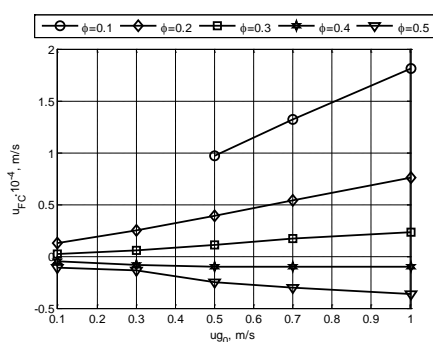


Figure 10: Combustion front velocity as function of gas entry velocity and equivalence ratio, $R_I = 0.02m$ and $h_{cool} = 400 \text{ W/m}^2/\text{K}$

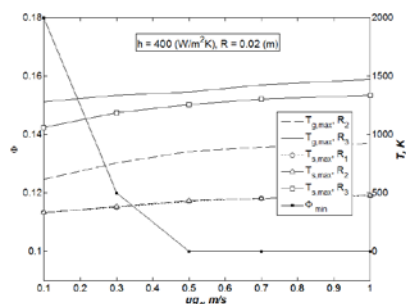


Figure 11: Combustibility limits (values of Φ_{min}) and maximum gas (dotted lines) and solid (solid lines) temperatures within the reactor at R_1, R_2 and R_3 ; $R_I = 0.02m$ and $h_{cool} = 400 \text{ W/m}^2/\text{K}$.

The comparison between figures 7 and 11 shows that increasing radius R_I from 0.01 to 0.02m significantly affects the combustibility limits of the mixture. If in the case $R_I = 0.01m$ the combustibility limits values are lowered from $\Phi_{min} = 0.1$ for $u_{g0} = 0.1 \text{ m/s}$ to $\Phi_{min} = 0.06$ for $u_{g0} = 1.0 \text{ m/s}$, in the case $R_I = 0.02m$, the same limits decrease from 0.18 to 0.1, within the same variation range of u_{g0} . Additionally, in the interval $0.5 < u_{g0} < 1.0$, the values of Φ_{min} are practically the same. The same figures also show that as radius R_I increased from 0.01 to 0.02m, the inside cylinder temperatures of the solid phase in R_1 and R_2 do not suffer major changes. Only for $u_{g0} > 0.5$, the temperatures in the

case $R_I = 0.02m$ are slightly higher ($\sim 25^\circ\text{C}$) than in the case $R_I = 0.01m$. These differences are stronger for higher values of u_{g0} . The same tendency is observed for gas temperatures in $r = R_2$: they have higher values in the case $R_I = 0.02m$ and the differences between both cases increase for higher values of u_{g0} , up to $\Delta T = 100^\circ\text{C}$ for $u_{g0} = 1.0$. On the surface $r = R_3$, the temperatures of the porous media maintained the same values in both cases, according to the value of R_I . However, the gas temperatures of the same region, on average, were 100°C higher for the case $R_I = 0.02m$.

After analyzing the case with $R_I = 0.02m$ and $h_{cool} = 400 \text{ W/m}^2/\text{K}$, the value of h_{cool} was varied, first considering $h_{cool} = 800 \text{ W/m}^2/\text{K}$ and later, $h_{cool} = 1500 \text{ W/m}^2/\text{K}$, for the same value of R_I , just like in the case of $R_I = 0.01m$. As a result, it was found that both combustion front velocity and combustibility limits of the mixture were practically invariable for h_{cool} , therefore, only the case $h_{cool} = 1500 \text{ W/m}^2/\text{K}$ is presented here in figures 12 and 13, omitting the case $h_{cool} = 800 \text{ W/m}^2/\text{K}$. The comparison between figures 10, 11 with 12, 13 show that combustion front velocity, combustibility limits and temperatures in the cylinder surface insulated ($r = R_3$) have not suffered any important change in value. However, there is some decrease in values of gas temperature and the porous media near the interior cylinder ($r = R_2$): gas temperatures lowered by about 100°C and solids, by about 25°C .

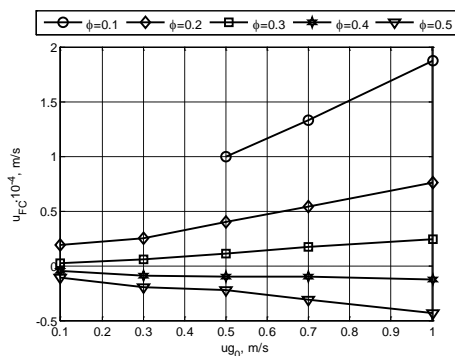


Figure 12: Combustion front velocity as function of gas entry velocity and equivalence ratio, $R_1 = 0.02m$ and $h_{cool} = 1500 W/m^2/K$.

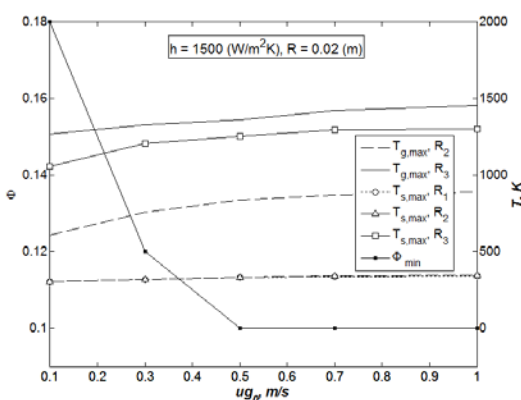


Figure 13: Combustibility limits (values of Φ_{min}) and maximum gas (dotted lines) and solid (solid lines) temperatures within the reactor at R_1, R_2 and R_3 ; $R_1 = 0.02m$ and $h_{cool} = 1500 W/m^2/K$.

As Figures 3, 8, 10 and 12 do not teach nulls of the combustion front velocity u_{FC} for different values of Φ , u_{g0} and h_{cool} , computer simulations were conducted to find their values. As a result, it was found that in the case with $R_1 = 0.02m$, $h_{cool} = 400 W/m^2/K$ and $u_{g0} = 0.1 m/s$, the u_{FC} speed was null for $\Phi = 0.328$. Increasing u_{g0} from 0.1 to 1.0 m/s for the same value of h_{cool} , the value of Φ for which $u_{FC} = 0$ increases, reaching $\Phi = 0.375$. Increasing the value of h_{cool} from 400 to 1500 $W/m^2/K$ does not show considerable variations in the value of Φ for which $u_{FC} = 0$. However, decreasing the value of R_1 from 0.02 to 0.01 m/s for all the values of h_{cool} and u_{g0} , the values of Φ for which $u_{FC} = 0$ resulted lower. Particularly, in the case of $u_{g0} = 0.1 m/s$ and $h_{cool} = 400 W/m^2/K$ the result is $u_{FC} = 0$ when $\Phi = 0.276$. By increasing u_{g0} to 1.0 m/s the value of Φ increases and reaches 0.368. It is also noted that by varying h_{cool} from 400 to 1500 $W/m^2/K$ for the same gas filtration velocity, the values of Φ were practically unchanged.

5. Conclusion

Computer simulations of combustion waves in annular cylindrical porous media show that, as in the case of porous cylindrical media, combustion waves are spread at a speed of around $10^{-4} m/s$, within the variation ranges of u_{g0} and Φ considered in this work. Depending on the value of the fuel equivalence ratio Φ , these waves may move upstream, in subadiabatic regime (for greater values of Φ), or downstream, in superadiabatic regime (for lower Φ) where the thermal and combustion wave travel in the same direction (downstream) along the porous media. For the same value of Φ , when the gas filtration velocity increases, the combustion wave travels at higher speeds in the superadiabatic regime, with their values unchanged or slightly decreasing in subadiabatic regime. It is also observed that along the complete variation interval of gas entry speed $0.1 < u_{g0} < 1.0 m/s$ the combustion front velocity has the same sign, positive or negative, if Φ is held constant. The variation of the radius in the inner cylinder noticeably affects the combustion characteristics, however, the heat loss from the inner cylinder have little effect on these, within the variation range of the considered parameters.

Acknowledgements - The support of CONICYT – Chile under FONDECYT Project 1131156, and of the Academia Politécnica Aeronáutica, FACH, Chile, is gratefully acknowledged.

References

- [1] S. Mößbauer, O. Pickenäcker, K. Pickenäcker, D. Trimis, Application of the porous burner technology in energy and heat engineering, in: Fifth International Conference on Technologies and Combustion for a Clean Environment (Clean Air V), Lisbon, Portugal, vol. 1, Lecture 20.2, 1999, pp. 519–523.
- [2] Valeri I. Bubnovich, Mario Toledo, Experimental study of a diluted methane–air mixture combustion under filtration in a packed bed, IASME Trans. 1 (3) (2004) 574–577.
- [3] W.M. Mathis Jr., J.L. Ellzey, Flame stabilization operating range and emissions for a methane/air porous burner, Combust. Sci. Technol. 175 (2003) 825–839.
- [4] D. Trimis, F. Durst, Combustion in a porous medium—advances and applications, Combust. Sci. Technol. 121 (1997) 153–168.
- [5] Mario Toledo, Valeri Bubnovich, Alexei Saveliev, Lawrence Kennedy, Filtration combustion of methane, ethane, and propane mixtures with air, WSEAS Trans. Heat Mass Transfer 1 (3) (2006) 283–292.
- [6] K.V. Dobrego, N.N. Gnesdilov, I.M. Kozlov, V.I. Bubnovich, H.A. Gonzalez, Numerical investigation of the new regenerator–recuperator scheme of VOC

- oxidizer, *Int. J. Heat Mass Transfer* 48 (2005) 4695–4703.
- [7] Nelson O. Moraga, César E. Rosas, Valeri I. Bubnovich, José R. Tobar, Unsteady fluid mechanics and heat transfer study in a double-tube air–combustor heat exchanger with porous medium, *Int. J. Heat Mass Transfer* 52 (2009) 3353–3363.
- [8] V.S. Babkin, Filtrational combustion of gases. Present state of affairs and prospects, *Pure Appl. Chem.* 65 (2) (1993) 335–344.
- [9] J.R. Howell, M.J. Hall, J.L. Ellzey, Combustion of hydrocarbon fuel within porous inert media, *Prog. Energy Combust. Sci.* 22 (1996) 121–145.
- [10] V. Bubnovich, L. Henríquez, N. Gnesdilov, Numerical study of the effect of the diameter of alumina balls on flame stabilization in a porous media burner, *Numer. Heat Transfer A, Appl.* 52 (3) (2007) 275–295.
- [11] V. Bubnovich, M. Toledo, L. Henríquez, C. Rosas, J. Romero, Flame stabilization between two beds of alumina balls in a porous burner, *Appl. Therm. Eng.* 30 (2010) 92–95.
- [12] V.S. Babkin, A.A. Korzhavin, V.A. Bunev, Propagation of premixed gaseous explosion flames in porous media, *Combust. Flame* 87 (1991) 182–190.
- [13] G. Brenner, K. Pickenäcker, O. Pickenäcker, D. Trimis, K. Wawrzinek, T. Weber, Numerical and experimental investigation of matrix-stabilized methane/air combustion in porous inert media, *Combust. Flame* 123 (2000) 201–213.
- [14] P.H. Bouma, L.P.H. De Goey, Premixed combustion on ceramic foam burners, *Combust. Flame* 119 (1999) 133–143.
- [15] J.G. Hoffmann, R. Echigo, H. Yoshida, S. Tada, Experimental study on combustion in porous media with a reciprocating flow system, *Combust. Flame* 111 (1997) 32–46.
- [16] F. Contarin, A.V. Saveliev, A.A. Fridman, L.A. Kennedy, A reciprocal flow filtration combustor with embedded heat exchangers: numerical study, *Int. J. Heat Mass Transfer* 46 (2003) 949–961.
- [17] Valeri Bubnovich, Luis Henriquez, Catalina Diaz, Emilio Avila, Stabilization operation region for a reciprocal flow burner, recent advances in applied and theoretical mechanics, in: *Proceedings of the Fifth WSEAS International Conference on Applied and Theoretical Mechanics (Mechanics'09)*, Puerto De La Cruz, Tenerife, Canary Islands, Spain, December 14–16, 2009, pp. 114–119.
- [18] Mao-Zhao Xie, Jun-Rui Shi, Yang-Bo Deng, Hong Liu, Lei Zhou, You-Ning Xu, Experimental and numerical investigation on performance of porous medium burner with reciprocating flow, *Fuel* 88 (2009) 206–213.
- [19] F. Contarin, W.M. Barcellos, A.V. Saveliev, L.A. Kennedy, Energy extraction from a porous media reciprocal flow burner with embedded heat exchangers, *Heat Mass Transfer* 127 (2) (2005) 123–130.
- [20] S. A. Zhdanok, K. V. Dobrego, S. I. Foutko, Flame localization inside axisymmetric cylindrical and spherical porous media burners, *Int. J. Heat Mass Transfer* 41 (1998) 3647–3655.
- [21] S. Zhdanok, L.A. Kennedy, G. Koester, Superadiabatic combustion of methane air mixtures under filtration in a packed bed, *Combust. Flame* 100 (1995) 221–231.
- [22] K. Hanamura, R. Echigo, Superadiabatic combustion in a porous medium, *Int. J. Heat Mass Transfer* 36 (13) (1993) 3201–3209.
- [23] Serguei I. Foutko, Stanislav I. Shabunya, and Serguei A. Zhdanok, Superadiabatic combustion wave in a diluted methane-air mixture under filtration in a packed bed, *Twenty-Sixth Symposium (International) on Combustion/The Combustion Institute, Pittsburgh*, (1996) 222–227.
- [24] Michael R. Henneke, and Janet L. Ellzey, Modeling of Filtration Combustion in a Packed Bed, *Combustion and Flame*, 117 (1999) 832–840.